CHALMERS

Chalmers Publication Library

The Silicon Trypanosome: A Test Case of Iterative Model Extension in Systems Biology

This document has been downloaded from Chalmers Publication Library (CPL). It is the author´s version of a work that was accepted for publication in:

Advances in Microbial Systems Biology

Citation for the published paper:
Achcar, F. ; Fadda, A. ; Haanstra, J. (2014) "The Silicon Trypanosome: A Test Case of Iterative Model Extension in Systems Biology". Advances in Microbial Systems Biology, vol. 64 pp. 115-143.

http://dx.doi.org/10.1016/b978-0-12-800143-1.00003-8

Downloaded from: http://publications.lib.chalmers.se/publication/201828

Notice: Changes introduced as a result of publishing processes such as copy-editing and formatting may not be reflected in this document. For a definitive version of this work, please refer to the published source. Please note that access to the published version might require a subscription.

Chalmers Publication Library (CPL) offers the possibility of retrieving research publications produced at Chalmers University of Technology. It covers all types of publications: articles, dissertations, licentiate theses, masters theses, conference papers, reports etc. Since 2006 it is the official tool for Chalmers official publication statistics. To ensure that Chalmers research results are disseminated as widely as possible, an Open Access Policy has been adopted.
The CPL service is administrated and maintained by Chalmers Library.

(article starts on next page)

CHAPTER THREE

The Silicon Trypanosome: A Test Case of Iterative Model Extension in Systems Biology

Fiona Achcar[*], Abeer Fadda[†], Jurgen R. Haanstra[‡,§], Eduard J. Kerkhoven[¶,||], Dong-Hyun Kim[¶], Alejandro E. Leroux[#], Theodore Papamarkou[**], Federico Rojas[††], Barbara M. Bakker[‡], Michael P. Barrett[¶], Christine Clayton[†], Mark Girolami[**], R. Luise Krauth-Siegel[#], Keith R. Matthews[††], Rainer Breitling[‡‡,1]

[*]Institute of Molecular, Cell and Systems Biology, College of Medical, Veterinary and Life Sciences, University of Glasgow, Glasgow, United Kingdom
[†]Zentrum für Molekulare Biologie der Universität Heidelberg, DKFZ-ZMBH Alliance, Heidelberg, Germany
[‡]Department of Pediatrics, Centre for Liver Digestive and Metabolic Diseases, and Systems Biology Centre for Energy Metabolism and Ageing, University Medical Center Groningen, University of Groningen, Groningen, The Netherlands
[§]Department of Molecular Cell Physiology, Faculty of Earth and Life Sciences, VU University Amsterdam, Amsterdam, The Netherlands
[¶]Wellcome Trust Centre for Molecular Parasitology, Institute of Infection, Immunity and Inflammation, and Glasgow Polyomics, College of Medical, Veterinary and Life Sciences, University of Glasgow, Glasgow, United Kingdom
[||]Systems and Synthetic Biology Group, Department of Chemical and Biological Engineering, Chalmers University of Technology, Gothenburg, Sweden
[#]Biochemie-Zentrum der Universität Heidelberg, Heidelberg, Germany
[**]The Department of Statistical Science and The Centre for Computational Statistics and Machine Learning University College London, London, United Kingdom
[††]Centre for Immunity, Infection and Evolution, Institute for Immunology and Infection Research, School of Biological Sciences, Ashworth Laboratories, University of Edinburgh, Edinburgh, United Kingdom
[‡‡]Manchester Institute of Biotechnology, Faculty of Life Sciences, University of Manchester, Manchester, United Kingdom
[1]Corresponding author: e-mail address: rainer.breitling@manchester.ac.uk

Contents

1. Introduction 116
2. Uncertainty in the Glycolysis Model 118
   2.1 Parameter uncertainty in the glycolysis model 118
   2.2 Topological uncertainty in the glycolysis model 123
3. Metabolic Extensions of the Model 125
   3.1 The pentose phosphate pathway 125
   3.2 The trypanothione pathway 127
4. Transcription/Translation Extensions of the Model 130
   4.1 The pre-mRNA-processing rates 131
   4.2 mRNA decay rates 132

Advances in Microbial Physiology, Volume 64
ISSN 0065-2911
http://dx.doi.org/10.1016/B978-0-12-800143-1.00003-8

© 2014 Elsevier Ltd
All rights reserved.

5. Experimental Data to Reduce Model Uncertainty and Refine Predictions 133
5.1 Measurements of concentrations and fluxes 133
5.2 Perturbations: RNAi cell lines 134
6. Conclusion 138
Acknowledgements 140
References 140

Abstract

The African trypanosome, *Trypanosoma brucei*, is a unicellular parasite causing African Trypanosomiasis (sleeping sickness in humans and nagana in animals). Due to some of its unique properties, it has emerged as a popular model organism in systems biology. A predictive quantitative model of glycolysis in the bloodstream form of the parasite has been constructed and updated several times. The Silicon Trypanosome is a project that brings together modellers and experimentalists to improve and extend this core model with new pathways and additional levels of regulation. These new extensions and analyses use computational methods that explicitly take different levels of uncertainty into account. During this project, numerous tools and techniques have been developed for this purpose, which can now be used for a wide range of different studies in systems biology.

1. INTRODUCTION

Trypanosoma brucei, a unicellular bloodstream parasite transmitted by tsetse flies, is the causative agent of African Trypanosomiasis (sleeping sickness in humans and nagana in animals; Barrett et al., 2003). In recent years, it has emerged as a popular model organism in systems biology (Barrett, Bakker, & Breitling, 2010), due to the wealth of information obtained in biomedical studies and the many advantages it offers: reproducible cultivation methods exist and quantitative analysis is well established. A quantitative mathematical model of central energy metabolism in the bloodstream form of the parasite was one of the first predictive kinetic models of a complex biological system (Bakker, Michels, Opperdoes, & Westerhoff, 1997), and this model has been iteratively updated after experimental testing and validation (Albert et al., 2005; Bakker et al., 2000; Bakker, Michels, Opperdoes, & Westerhoff, 1999; Haanstra, van Tuijl, et al., 2008; Helfert, Estévez, Bakker, Michels, & Clayton, 2001), yielding one of the most extensively curated kinetic metabolic models currently available.

The Silicon Trypanosome (SilicoTryp) is a project that brings together computational systems biologists and trypanosome experts to address

multi-level regulation of trypanosome physiology on a new scale. Using a Bayesian approach that explicitly takes multiple levels of uncertainty into account, the project aims at re-analysing the core model of glycolysis and extends it in two directions: metabolic extensions towards new pathways ("horizontal" extensions) and inclusion of transcription and translation ("vertical" extensions). Explicitly including our uncertainty, both in the parameter values and the topologies of the different extensions, allows us not only to quantify our level of confidence in the results but also to determine, in an unbiased manner, pitfalls and inconsistencies that might have gone unnoticed if the modelling was done without uncertainty awareness.

The horizontal extensions initially focus on the pathways controlling redox balance in trypanosomes: the trypanothione pathway, which is critical for parasite survival in the host, and the pentose phosphate pathway that links the trypanothione pathway to glycolysis by providing the necessary NADPH. Adding these two pathways requires knowledge of the kinetic parameters of all enzymes involved. In order to obtain the most accurate parameter values for these additional enzymes, a new buffer was developed to mimic as closely as possible the conditions in the cytosol of the parasite, as has previously been done for yeast (van Eunen et al., 2010). The first enzyme characterised in this buffer was trypanothione synthetase, the final enzyme of the trypanothione biosynthesis pathway, using a method that integrates laboratory experimentation and modelling to explore alternative model topologies (Leroux, Haanstra, Bakker, & Krauth-Siegel, 2013).

In addition to these metabolic extensions, the SilicoTryp project aims at a vertical extension of the model by including additional levels of control: transcription and translation. In trypanosomes, transcription rates (with very few exceptions) play little role in the regulation of mRNA concentrations since transcription by RNA polymerase II is not regulated for individual genes (Siegel, Gunasekera, Cross, & Ochsenreiter, 2011). Instead, regulation is achieved at the levels of pre-mRNA- and mRNA-processing and degradation. These levels of control are modelled based on the previously published ordinary differential equations model of phosphoglycerate kinase (PGK) transcription and translation (Haanstra, Stewart, et al., 2008). The necessary parameters are acquired using deep sequencing (RNAseq). These estimates will be particularly uncertain, compared to metabolic enzyme parameters, and this provides an additional motivation for using a fully uncertainty-aware modelling strategy.

The uncertainty-aware modelling requires a rigorous method for updating our initial (prior) beliefs on the parameter values of the models,

when new data becomes available. For this purpose, it was necessary to develop a computationally efficient Monte Carlo variance reduction method (Papamarkou, Mira, & Girolami, 2014). Two types of large-scale experimental data are generated within the SilicoTryp project to drive the iterative updating process: steady-state concentration of metabolites and metabolic fluxes were measured using liquid chromatography–mass spectrometry (LC–MS) in standard conditions, and a collection of RNAi mutants were constructed, to examine the behaviour of the system under a variety of perturbations. The mutants in this collection will be characterised at the metabolome, transcriptome and proteome level, providing new data to further refine the extended model and reduce our uncertainty on model topology and parameter values.

2. UNCERTAINTY IN THE GLYCOLYSIS MODEL

SilicoTryp explicitly deals with uncertainty at multiple levels (experimental data, kinetic parameter values, model topology) in every aspect of the project. It aims at applying the general framework of Fig. 3.1 (Vyshemirsky & Girolami, 2008; Xu et al., 2010).

The *T. brucei* glycolysis model, as previously published (Albert et al., 2005; Bakker et al., 2000, 1997; Bakker, Michels, et al., 1999; Haanstra, van Tuijl, et al., 2008; Helfert et al., 2001) (Fig. 3.2), used a single set of parameters values. Some basic uncertainty analysis was included by scanning a range of values for selected parameters individually (Bakker et al., 1997) or comparing two alternative topologies (Bakker, Michels, et al., 1999), but the combined effect of uncertainty in *all* parameters was not evaluated systematically, nor were the plausible distributions of parameter values explicitly defined. Therefore, an important step in the SilicoTryp project was to collect information not only on the (experimental and biological) uncertainty of all parameter values in the previously published model but also on the uncertainty of the topology of the metabolic network.

2.1. Parameter uncertainty in the glycolysis model

In order to evaluate uncertainty on the parameter values of the glycolysis model, a Mediawiki-based website was created, the SilicoTryp wiki (http://silicotryp.ibls.gla.ac.uk/wiki). In this wiki, the sources and calculations underlying the values for every parameter of the glycolysis model were documented (see e.g. in Fig. 3.3). This detailed source of documentation allowed us to define probability distributions for each parameter, hence

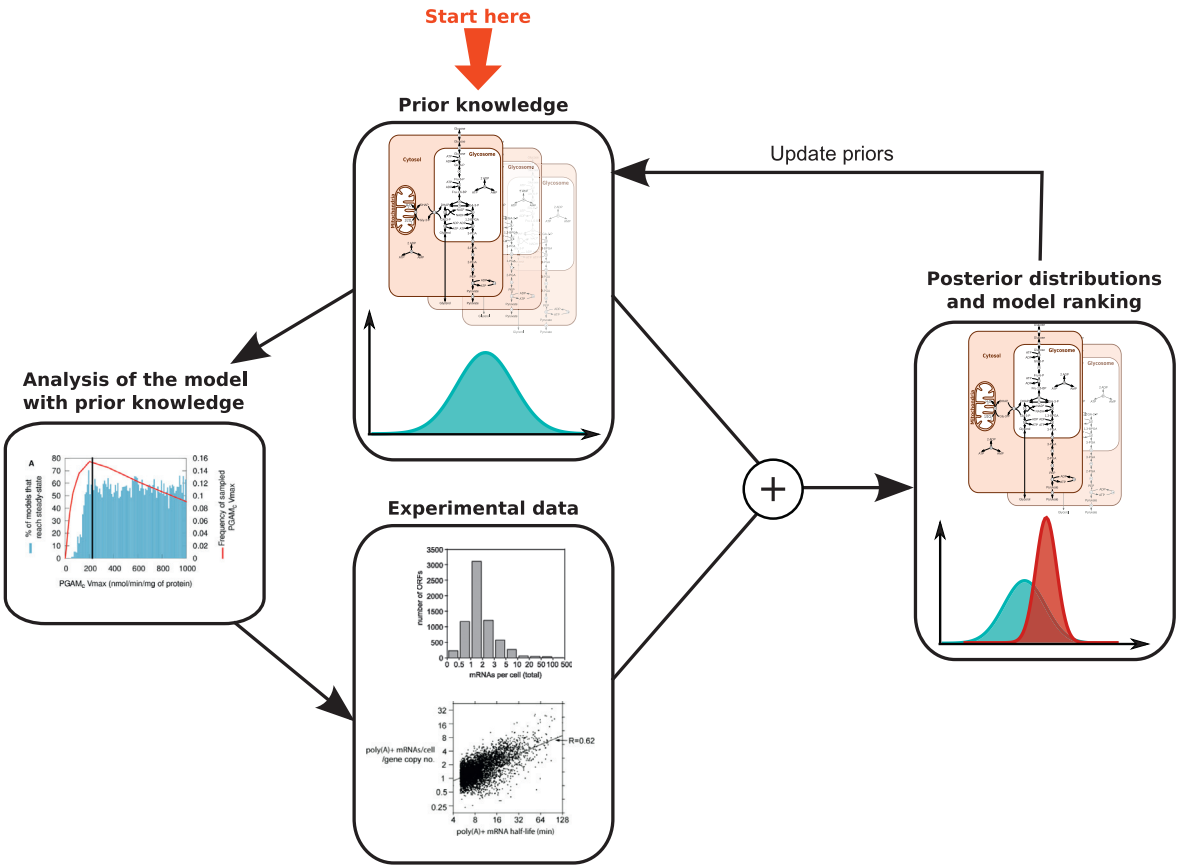

Figure 3.1 General Bayesian framework for explicitly handling uncertainty in the SilicoTryp project.

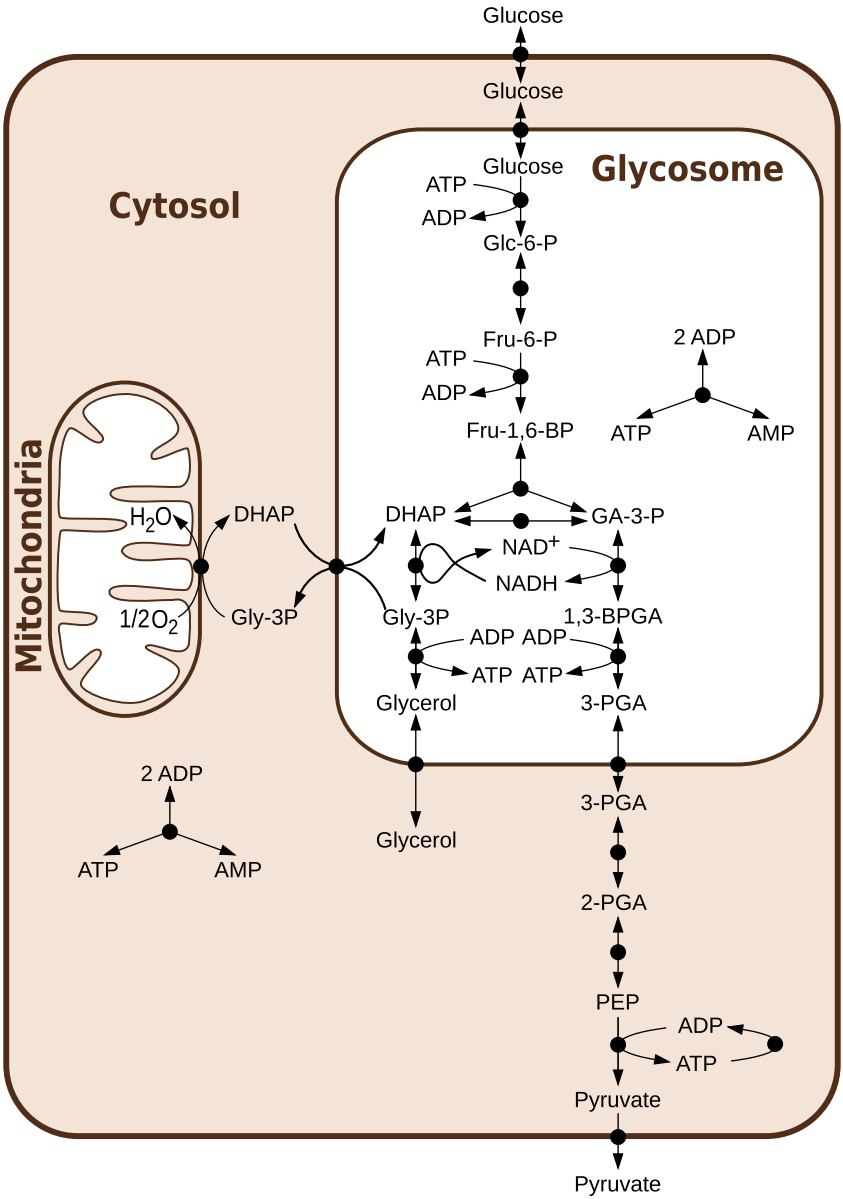

Figure 3.2 Glycolysis in T. *brucei* as previously published (Albert et al., 2005). *Abbreviations*: Glc-6-P, glucose 6-phosphate; Fru-6-P, fructose 6-phosphate; Fru-1,6-BP, fructose 1,6-bisphosphate; DHAP, dihydroxyacetone phosphate; GA-3-P, glyceraldehyde 3-phosphate; Gly-3-P, glycerol 3-phosphate; 1,3-BPGA, 1,3-bisphosphoglycerate; 3-PGA, 3-phosphoglycerate; 2-PGA, 2-phosphoglycerate; PEP, phosphoenolpyruvate. *Reprinted from Achcar et al. (2012), under the Creative Commons Attribution License.*

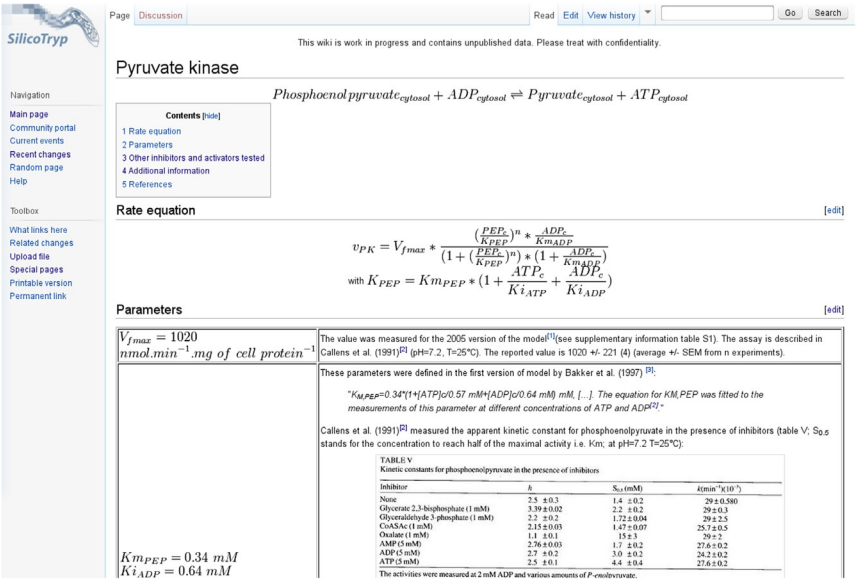
SilicoTryp

Page Discussion Read Edit View history Go Search

This wiki is work in progress and contains unpublished data. Please treat with confidentiality.

Navigation
Main page
Community portal
Current events
Recent changes
Random page
Help

Toolbox
What links here
Related changes
Upload file
Special pages
Printable version
Permanent link

Pyruvate kinase

$$Phosphoenolpyruvate_{cytosol} + ADP_{cytosol} \rightleftharpoons Pyruvate_{cytosol} + ATP_{cytosol}$$

Contents [hide]
1 Rate equation
2 Parameters
3 Other inhibitors and activators tested
4 Additional information
5 References

Rate equation [edit]

$$v_{PK} = V_{fmax} * \frac{(\frac{PEP_c}{K_{PEP}})^n * \frac{ADP_c}{Km_{ADP}}}{(1+(\frac{PEP_c}{K_{PEP}})^n) * (1+\frac{ADP_c}{Km_{ADP}})}$$

with $K_{PEP} = Km_{PEP} * (1 + \frac{ATP_c}{Ki_{ATP}} + \frac{ADP_c}{Ki_{ADP}})$

Parameters [edit]

$V_{fmax} = 1020$ $nmol.min^{-1}.mg\ of\ cell\ protein^{-1}$	The value was measured for the 2005 version of the model[1](see supplementary information table S1). The assay is described in Callens et al. (1991)[2] (pH=7.2, T=25°C). The reported value is 1020 +/- 221 (4) (average +/- SEM from n experiments).
$Km_{PEP} = 0.34\ mM$ $Ki_{ADP} = 0.64\ mM$	These parameters were defined in the first version of model by Bakker et al. (1997) [3]; "$K_{M,PEP}$=0.34*(1+[ATP]c/0.57 mM+[ADP]c/0.64 mM) mM, [...]. The equation for KM,PEP was fitted to the measurements of this parameter at different concentrations of ATP and ADP[2]." Callens et al. (1991)[2] measured the apparent kinetic constant for phosphoenolpyruvate in the presence of inhibitors (table V; $S_{0.5}$ stands for the concentration to reach half of the maximal activity i.e. Km; at pH=7.2 T=25°C):

TABLE V
Kinetic constants for phosphoenolpyruvate in the presence of inhibitors

Inhibitor	h	$S_{0.5}$ (mM)	k(min^{-1})(10^{-3})
None	2.5 ±0.3	1.4 ±0.2	29±0.580
Glycerate 2,3-bisphosphate (1 mM)	3.39±0.02	2.2 ±0.2	29±0.3
Glyceraldehyde 3-phosphate (1 mM)	2.2 ±0.2	1.72±0.04	29±2.5
CoASAc (1 mM)	2.15±0.03	1.47±0.07	25.7±0.5
Oxalate (1 mM)	1.1 ±0.1	15±3	29±2
AMP (5 mM)	2.76±0.03	1.7 ±0.2	27.6±0.2
ADP (5 mM)	2.7 ±0.2	3.0 ±0.2	24.2±0.2
ATP (5 mM)	2.5 ±0.1	4.4 ±0.4	27.6±0.2

The activities were measured at 2 mM ADP and various amounts of P-enolpyruvate.

Figure 3.3 Example page of the SilicoTryp wiki. Chemical and rate equations are described, and sources for each parameter are documented in detail.

representing our prior beliefs on what the true parameter values are (Achcar et al., 2012).

Using these distributions, sets of plausible parameters were sampled. A large collection of variant models, each with a different set of sampled parameters, was then simulated, allowing us to quantify confidence intervals for different model properties, such as steady-state concentrations and fluxes or control coefficients resulting from the parameter uncertainty (see Fig. 3.4). This strategy allowed us not only to gain knowledge on how confident we are about the model predictions but also to detect fragilities of the model in an unbiased way, highlighting areas of the model behaviour that are in contradiction with experimental data (Achcar et al., 2012). We showed, for example, that only in 40% of our sampled models is the control over the glucose consumption flux mostly held by the glucose transporter, as described before with the fixed parameter model (Bakker, Michels, et al., 1999; Bakker, Walsh, et al., 1999). In the equally plausible scenarios represented by the remaining 60% of the models, this control is shared between several other glycolytic enzymes, and which enzymes share control over the glucose consumption flux depends on the parameter sets considered (Achcar et al., 2012).

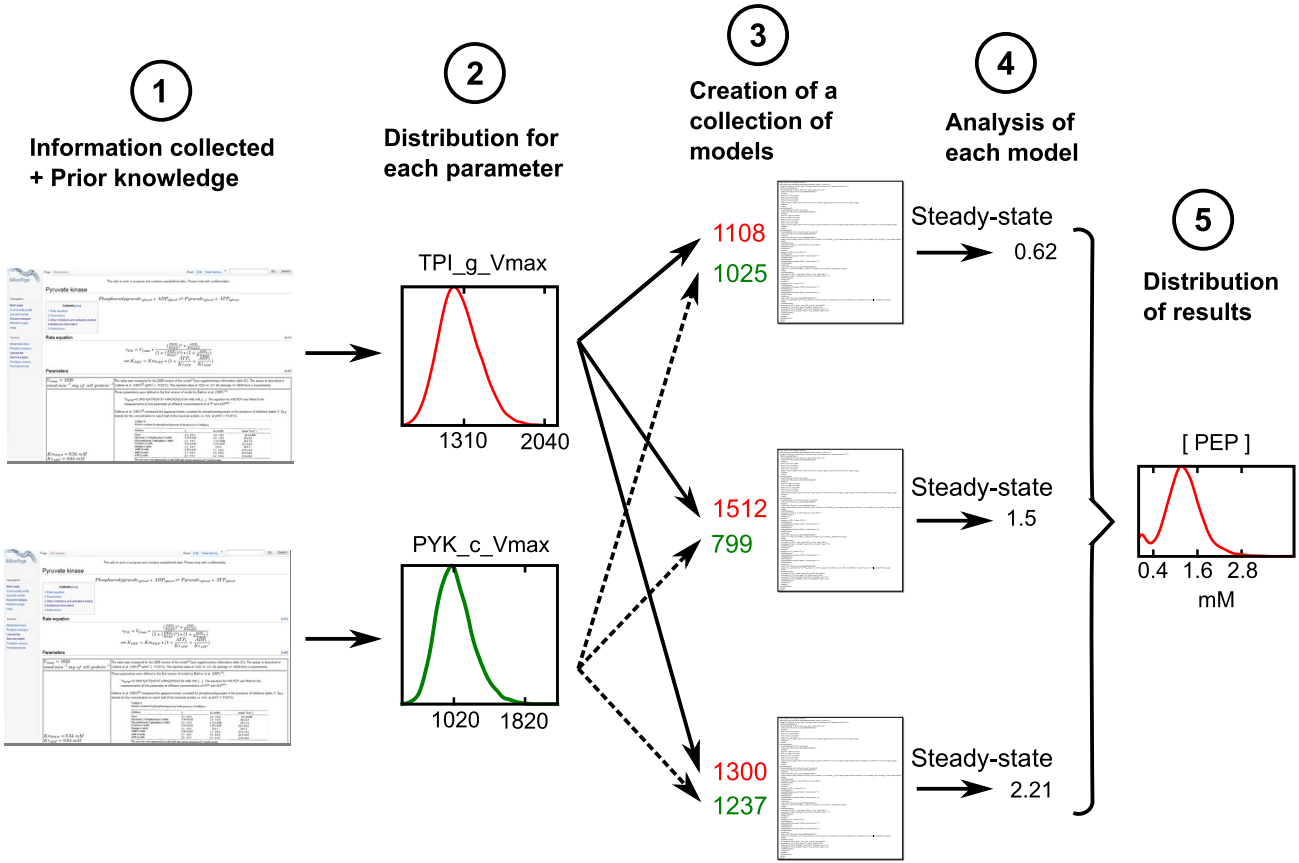

Figure 3.4 Evaluation of parameter uncertainties and their effect on the model results. *Reprinted with permission from Breitling, Achcar, and Takano (2013). Copyright 2013 American Chemical Society.*

2.2. Topological uncertainty in the glycolysis model

In addition to evaluating the effect of parameter value uncertainty, we explored the effect of topological uncertainty in the glycolysis model (Xu et al., 2010). Although *T. brucei* central energy metabolism has been exceptionally well studied for a long time, some areas of its network connectivity remain controversial. Indeed, the previously published model considered the glycosomes, organelles where most of the glycolytic enzymes are localised (see Fig. 3.2), as impermeable compartments into which all required metabolites need to be transported via specific transporters. This hypothesis was reinforced by both theoretical (Bakker et al., 2000) and experimental (Haanstra, van Tuijl, et al., 2008) findings that mislocalising the glycolytic enzymes to the cytosol causes a lethal accumulation of sugar phosphate. This confirmation of theoretical predictions by experimental results has been considered one of the major successes of the *T. brucei* glycolysis model.

However, recently, size-specific pores have been discovered in the glycosomal membrane (Gualdron-López et al., 2012). These pores are essentially chemically non-selective holes and their presence implies that small metabolites can diffuse freely across the membrane, while only the largest molecules would be retained inside the glycosomes. This creates additional potential links in the metabolic network, between cytosol and glycosome, which are not yet fully understood, but need to be considered in the metabolic modelling.

Another aspect of topological uncertainty is due to the fact that we know that enzymes are imported into the glycosome fully folded (Häusler, Stierhof, Wirtz, & Clayton, 1996; Michels et al., 2005); of course, these might be fully sequestered in transit by the protein import machinery, but there is also a concrete possibility that there could be some residual activity of glycosomal glycolytic enzymes in the cytosol. Cytosolic activity of the relevant enzymes has so far been poorly characterised and is generally neglected in modelling.

To test the effect of increasing permeability of the glycosome, a series of models was constructed (Achcar, Barrett, & Breitling, 2013). These models have increasingly permeable glycosomes, ranging from the impermeable glycosomes of the previous models (model 1a has a similar topology as the models published since 1999 (Bakker, Michels, et al., 1999), model 1b has a similar topology as the model of 1997 (Bakker et al., 1997)) to glycosomes permeable to all metabolites up to the size of ATP (model 6).

For each of these models, the uncertainty on the parameter values was taken into account as previously (Achcar et al., 2012). This was then extended by also including the uncertainty on the percentage of activity of the glycosomal enzymes in the cytosol. The resulting collection of models was simulated, and results were compared to experimental data (metabolite concentrations and fluxes) by computing log-likelihoods: the higher the log-likelihoods the better the match between simulations and experiments (see Fig. 3.5). Our results show that, quite surprisingly, the semi-permeable models that let metabolites smaller than fructose 6-phosphate (model 3) or smaller than fructose 1,6-bisphosphate (model 4) freely diffuse, agree with the experimental data at least as well as the impermeable model (model 1a). This is consistent with the idea that only compartmentation of ATP is required. Contrary to the common intuition that organelles like the glycosome function as tightly sealed compartments, at least for glycosomal glycolysis a certain degree of leakiness for smaller metabolites appears to be fully compatible with its function.

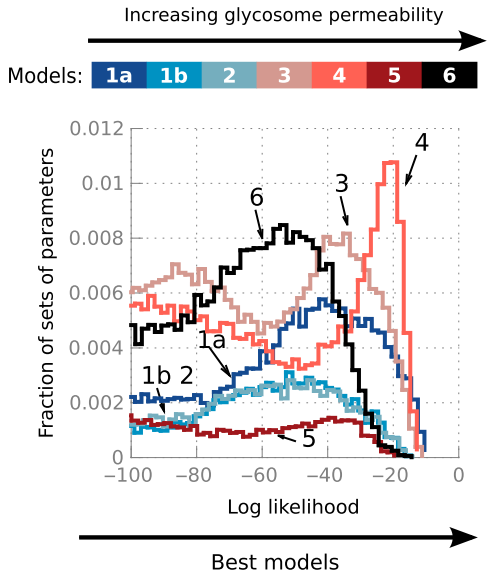

Figure 3.5 Log-likelihood (goodness of fit to experimental data) of models with increasing glycosome permeability and cytosolic activities of the glycosomal enzymes. The higher the log-likelihood, the better the match between simulations and experimental results. Each model is simulated with a range of parameter sets that describes our uncertainty about the parameter values. See Achcar et al. (2013) for details. *Modified with permission from Achcar et al. (2013). Copyright 2013 John Wiley and Sons.*

In addition, the analysis allowed us to show that, for all topologies with a semi-permeable glycosome tested, the fraction of residual cytosolic activity of some glycolytic enzymes probably plays a crucial role in explaining parasite physiology.

3. METABOLIC EXTENSIONS OF THE MODEL

With the uncertainty-aware model of central carbon metabolism established, the SilicoTryp project could aim at including the trypanothione and pentose phosphate pathways and the associated extra levels of uncertainty into the model.

3.1. The pentose phosphate pathway

In *T. brucei*, the pentose phosphate pathway is localised in both the cytosol and the glycosome where its presence breaks the bound-phosphate balance that was thought to be essential (Bakker et al., 2000; Haanstra, van Tuijl, et al., 2008). This phosphate "leak" needs to be solved either by finding a viable model that does not need bound-phosphate to be balanced in the glycosome, or by adding reactions to restore this balance. One solution within each of these two categories of solutions was tested (Kerkhoven et al., 2013).

The first solution tested maintained the bound-phosphate balance by adding ribokinase to the glycosome (hypothesis 1 of Fig. 3.6). In the context of impermeable glycosomes, ribokinase would work in the direction of producing ATP and ribose. To be able to model this solution, the enzyme was characterised biochemically (Kerkhoven et al., 2013). However, despite being sufficient theoretically, the results showed that this enzyme alone cannot maintain the bound-phosphate balance. The second solution modelled involves breaking the bound-phosphate balance by introducing an ATP/ADP translocator. However, modelling shows that this translocator would need to be very tightly regulated for the parasite to be viable. This makes it unlikely that such an antiporter alone could represent a solution and more reactions are probably involved in the regulation of the bound-phosphate balance.

Despite the topological uncertainty that remains, both of these model versions can already be used to some extent. Both of them handle oxidative stress in the same way, and the models have been used to test possible mechanisms to explain why the third enzyme of the PPP, 6-phosphogluconate dehydrogenase (from 6-PG to Rul-5-P in Fig. 3.6), is essential for parasite survival. The resulting predictions were then tested experimentally and it

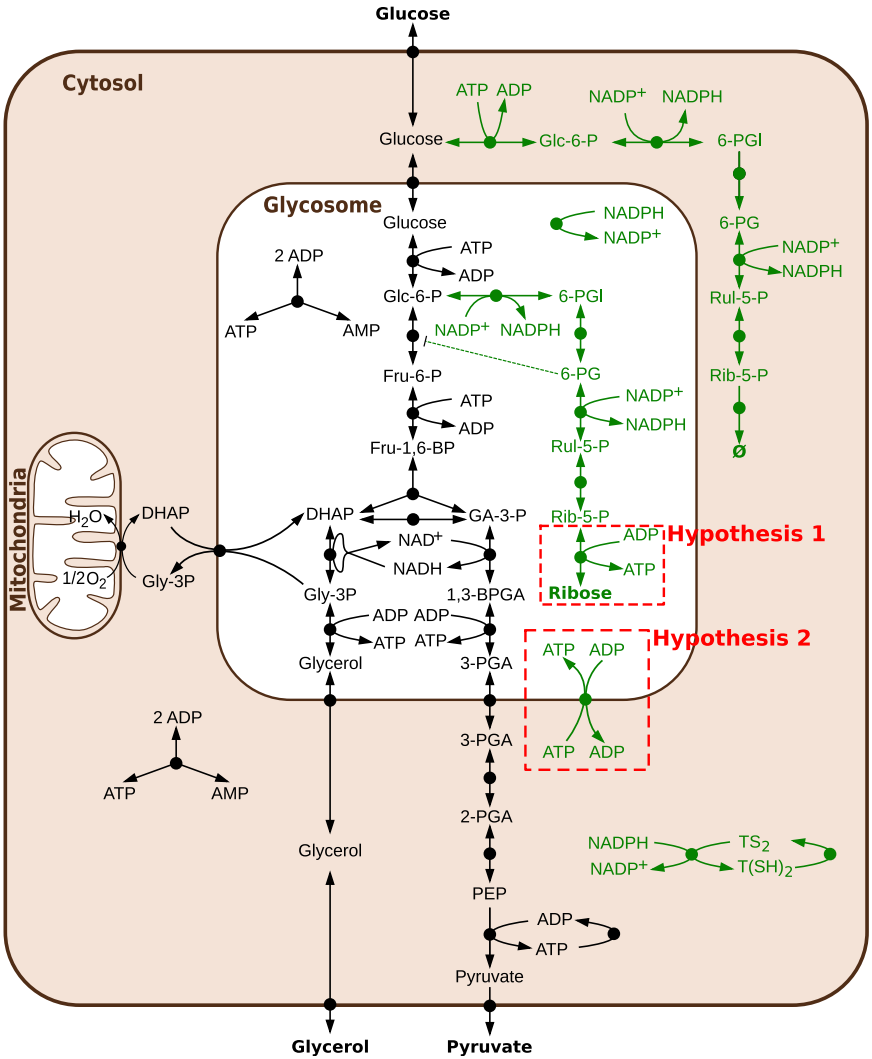

Figure 3.6 Two hypotheses tested to solve the topology of the pentose phosphate pathway. In black, the reactions of the glycolysis model, in grey the reactions introduced to model the pentose phosphate pathway. Abbreviations are not present in Fig. 3.2: 6-PGl, 6-phosphogluconolactone; 6-PG, 6-phosphogluconate; Rul-5-P, ribulose 5-phosphate; Rib-5-P, ribose 5-phosphate; TS_2, trypanothione disulfide; $T(SH)_2$, trypanothione.

was shown that a positive feedback loop related to 6-PG inhibition of phosphoglucose isomerase was not responsible for the 6-phosphogluconate dehydrogenase essentiality in *T. brucei* (Kerkhoven et al., 2013), in contrast to the situation in many other organisms.

3.2. The trypanothione pathway

3.2.1 The pathway topology

In order to extend the model with the trypanothione pathway, a main contributor to redox balance in *T. brucei*, we first had to determine the stoichiometric map of this pathway. We constructed a stoichiometric map of the trypanothione pathway based on the literature and LC–MS data (see Fig. 3.7). Cells were grown in the presence of 50% ^{13}C-labelled glucose over 48 h, after which their metabolites were extracted and analysed using LC–MS (Kim, D.H., Achcar, F. et al., in preparation). The partially labelled metabolome allowed us to rule out the presence of the methionine salvage pathway (marked 1 in Fig. 3.7) in *T. brucei*. Indeed, if this pathway—recycling methylthioadenosine (MTA) into methionine—was occurring, we should detect some four carbon-labelled methionine. However, methionine is clearly detected as fully unlabelled, indicating that the pathway is not complete (Kim, D.H., Achcar, F. et al., in preparation).

One question that remains open is the origin of ornithine *in vivo*. Previous data indicated that trypanosomes lack arginase (Vincent et al., 2012), the

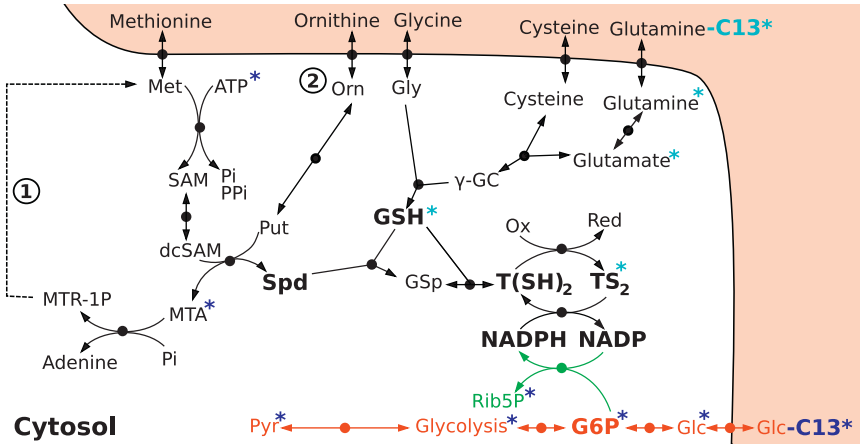

Figure 3.7 Stoichiometric map of the trypanothione pathway. The blue asterisks indicate which metabolites are found ^{13}C labelled when all glucose carbons are ^{13}C labelled. The turquoise asterisks indicate which metabolites are labelled when glutamine is labelled. The methionine salvage pathway, marked as 1, does not seem to be active in *T. brucei* (see text). The origin of ornithine, marked as 2, remains uncertain. *Abbreviations*: Orn, ornithine; Gly, glycine, Met, methionine; γ-GC, γ-glutamylcysteine; SAM, *S*-adenosylmethionine; dcSAM, decarboxylated *S*-adenosylmethionine; Spd, spermidine; Gsp, glutathionylspermidine; MTA, methylthioadenosine; MTR-1P, methylthioribose 1-phosphate; Glc, glucose; G6P, glucose 6-phosphate; Pyr, pyruvate; TS_2, trypanothione disulfide; $T(SH)_2$, trypanothione.

enzyme that produces ornithine from arginine, which is the common source of ornithine in eukaryotic cells including other parasites (Vincendeau, Gobert, Daulouède, Moynet, & Djavad Mossalayi, 2003). It was also shown that in the presence of ornithine, *T. brucei* is capable of using it directly, and therefore it was hypothesised that the cells use ornithine directly from the medium. However, measurements of the metabolite composition in the growth medium over time (Kim, D.H., Achcar, F. et al., in preparation; see below) showed that the ornithine concentration is quite low in the growth medium (Creek et al., 2013; see Section 5.2) and does not change over time (staying between 15 and 20 μM in the medium; it was measured as 54.4 ± 16.1 μM by Martens-Lobenhoffer et al. in blood (Martens-Lobenhoffer, Postel, Tröger, & Bode-Böger, 2007), i.e. the same order of magnitude). This suggests that there probably is another route to the production of ornithine in *T. brucei*, and its origin is currently being examined.

3.2.2 Uniform assay conditions

Usually, enzyme activities are measured under non-physiological optimum conditions. For a reliable in *silico* model and to reduce our uncertainty about the parameter values, the data should preferably be obtained under conditions that mimic the milieu in which the pathway is active in the cell (van Eunen et al., 2010). The importance of physiological conditions to measure metabolic functions was recently demonstrated: the use of an "*in vivo*-like" assay medium yielded enzyme kinetic parameters that substantially improved a computational model of yeast glycolysis (van Eunen, Kiewiet, Westerhoff, & Bakker, 2012). Such a buffer had not been used for *T. brucei* before. Based on the available literature, we therefore developed a new phosphate buffer system at pH 7.0 in which measurements are done at 37 °C (Table 3.1), mimicking the physiological environment of the enzymes in the cytosol of bloodstream-form parasites (Leroux et al., 2013).

3.2.3 A detailed focus on one enzyme: Trypanothione synthetase

We first employed our *in vivo*-like assay to characterise kinetically the enzyme of the final step in trypanothione ($T(SH)_2$) synthesis. *T. brucei* trypanothione synthetase (TryS) generates $T(SH)_2$ from glutathione (GSH) and spermidine (Spd) in two consecutive ATP-dependent reactions (Comini et al., 2004; Oza, Ariyanayagam, Aitcheson, & Fairlamb, 2003). In the first step, glutathionylspermidine (Gsp) is formed, which is then combined with a second GSH to yield $T(SH)_2$. *In vitro*, TryS also displays amidase activity and can, in total, catalyse five different reactions: ATP

Table 3.1 Characteristics of the *in vivo*-like buffer system for the cytosol of bloodstream *T. brucei*

Parameter	Value	Reference(s)
Temperature	37 °C	
pH	7.0	Nolan and Voorheis, (2000a) and Thissen and Wang (1991)
[Phosphate]	10 mM	Moreno et al. (2000)
$[K^+]$	100 mM	Nolan and Voorheis (2000b)
$[Na^+]$	15 mM	Nolan and Voorheis (2000b)
$[Mg^{2+}]$	10 mM	Fuad et al. (2011)
$[Cl^-]$	120 mM	Nolan and Voorheis (2000b)
Ionic strength	200 mM	

hydrolysis, formation of Gsp and $T(SH)_2$ as well as hydrolysis of the conjugates to regenerate GSH and Spd. As the mechanism of TryS is rather complex, a rate equation could not be easily formulated. To obtain a deeper insight in the exact molecular mechanism of the synthetase reactions of TryS, we formulated alternative kinetic models with different topologies of the catalytic cycle. Each elementary reaction step was modelled by a mass-action kinetic equation. The model parameters were then fitted by evolutionary programming to the extensive matrix of steady-state data obtained for different substrate/product combinations using our *in vivo*-like buffer. In the process of building the model, a strong interaction between experimental and modelling efforts proved to be essential. New enzyme kinetic experiments were designed to provide data to help discriminate between different models. Moreover, when the fit to the data was suboptimal model topology was adjusted in an iterative cycle (see Fig. 3.8).

The best model describes the full kinetic profile of TryS and is also able to predict time profiles of (intermediate) product formation that were not used in the fitting of the parameters, and thus serve as validation data (Leroux et al., 2013). It also provides a mechanism for inhibition by the substrate glutathione and the product trypanothione. In our *in vivo*-like assay, some of the kinetic constants proved markedly different from earlier measurements in other buffer systems (Oza et al., 2003; Torrie et al., 2009). Major alterations were a threefold higher K_i value for GSH, a rise of the K_m value for Spd from 139 to 687 μM and a reduction of the k_{cat} from 5.2 to 2.8 s^{-1}. These

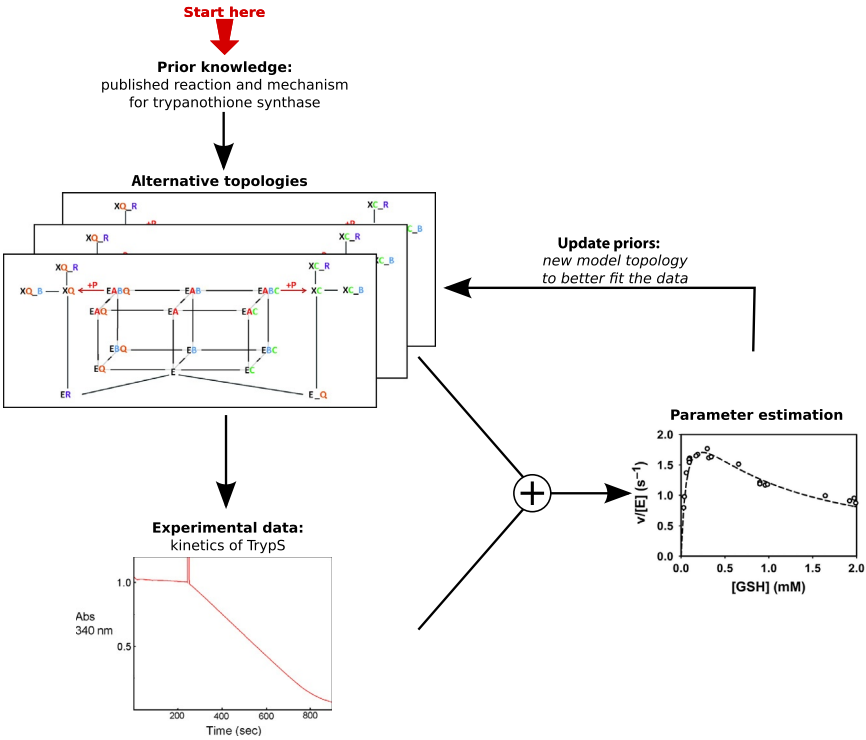

Figure 3.8 Workflow applied for dissecting the kinetic mechanism of trypanothione synthetase. *Modified with permission from Leroux et al. (2013). Copyright 2013 American Society for Biochemistry and Molecular Biology.*

observations are further demonstration of the importance of mimicking the physiological environment.

4. TRANSCRIPTION/TRANSLATION EXTENSIONS OF THE MODEL

One of the aims of the SilicoTryp project is to include transcription and translation in the model, resulting in dynamic enzyme levels, instead of using fixed V_{max} values for all enzymes. This will be done using a module of four differential equations for each enzyme (see Fig. 3.9), based on the previously published model of phosphoglycerol kinase transcription and translation (Haanstra, Stewart, et al., 2008). Regulation of enzyme concentrations in *T. brucei* is typically achieved by controlling the pre-mRNA-processing rate ($k_{splicing}$ in Fig. 3.9), the translation rate ($k_{translation}$) and/or

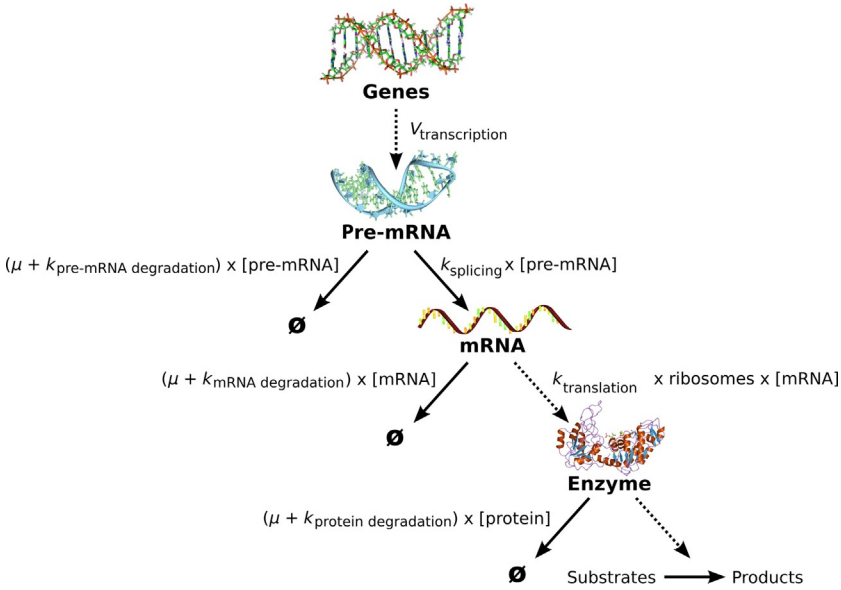

Figure 3.9 Transcription/translation module that will be added for every enzyme of the model. The module is based on the model published by Haanstra, Stewart, et al. (2008). The rate constants of the various processes involved are indicated by *k*, and μ are the specific growth rate of the trypanosomes, and *ribosomes* represents the number of ribosomes per molecule of mRNA.

the degradation rates. To measure the pre-mRNA and mRNA degradation and processing rates, RNAseq experiments were done and are currently being analysed.

4.1. The pre-mRNA-processing rates

Genes in trypanosomes are transcribed as polycistronic precursor messages (pre-mRNA) that are destined for either trans-splicing into mature mRNA or degradation. In order to measure the rate of pre-mRNA-processing for each gene, cells were treated with Actinomycin D for 5 min to inhibit mRNA transcription. RNA was then extracted and, after being depleted from rRNA, two biological replicates and two controls were subjected to transcriptome-wide deep sequencing (RNAseq, an average of 50 million reads of length 50mer, using Illumina HiSeq 2000). A decrease in pre-mRNA read counts in treated cells will be due to the splicing of the pre-mRNA in the absence of transcription. The ratio of pre-mRNA read counts (treated cells over untreated) was then used to estimate the rate of mRNA

processing. A difficulty in differentiating between reads from pre-mRNA sequences and those due to spurious transcription events in the same region, led us to limit our analysis to the 20 nucleotides immediately upstream of known splice acceptor sites. Although this had the drawback of limiting the number of examined regions, this filter increases our confidence about the origin of the reads.

Preliminary results indicate that 50% of the transcripts have a half-life of less than 2 min, but some showed much longer apparent half-lives. We speculate that this is due to persistence of bi-cistronic RNAs, perhaps in the cytoplasm (Fadda, A. et al., in preparation).

4.2. mRNA decay rates

In order to measure mRNA degradation rates, cells were treated with both Actinomycin D and Sinefungin to inhibit both transcription and splicing. RNA was extracted at several time points after transcription inhibition, depleted from rRNA and subjected to deep sequencing (an average of 25 million 75mer reads, or 200 million 50mer reads, using Illumina GAIIX and HiSeq 2000, respectively). Since all trypanosome mRNAs carry the same 39-nt spliced leader (SL) at the 5′-end, the abundance of the SL can serve as a proxy for the abundance of total mRNA. This allowed us to normalise the read counts using the total mRNA decay pattern across the same time points. Then, amounts of total mRNA were measured relative to the steady state (Fadda, Färber, Droll, & Clayton, 2013), and mRNA half-lives were first estimated using an exponential model.

It has been shown, however, that in a transcription inhibition experiment, while the majority of transcripts decay exponentially, others exhibit a slow-to-fast or fast-to-slow decay pattern. In our work, we see the same pattern. Therefore, we used a Markov chain model developed earlier by Deneke, Lipowsky, and Valleriani (2013) to analyse the data for transcripts that do not show exponential kinetics. Transcripts exhibiting non-exponential decay are presumed to be degraded in a multi-step reaction, in which more than one rate-limiting step exists, and where the age of the transcript becomes relevant to its rate of degradation. This is now further studied with a particular focus on the mRNAs encoding enzymes of the glycolytic and redox pathways, many of which show non-exponential decay.

The mRNA kinetic data are furthermore being complemented with information on the translation rates for each transcript, using a ribosome profiling (Ingolia, Ghaemmaghami, Newman, & Weissman, 2009) strategy.

The number of ribosomes on each mRNA is determined by treating cell lysates with RNase to digest the mRNA except those stretches protected by ribosomes. The protected RNA fragments are then purified and sequenced, and the rate of translation estimated by assuming a linear relationship between the ribosome number on a transcript and the rate of translation.

5. EXPERIMENTAL DATA TO REDUCE MODEL UNCERTAINTY AND REFINE PREDICTIONS

In order to reduce our uncertainty about both model topology and parameter values, further experimental data are needed, in addition to the transcription dynamics work described above. Data collection within SilicoTryp focused initially on steady-state metabolite concentrations and fluxes, which are directly informative for model refinement.

In addition, a collection of RNAi mutants was constructed with the aim of providing additional information on the system's behaviour upon perturbation.

5.1. Measurements of concentrations and fluxes

Intracellular and extracellular concentrations and fluxes were measured using LC–MS. However, mass spectrometry intensities are not always linearly proportional to the concentrations due to ion suppression effects (Annesley, 2003). In addition, variations in instrumental response and degradation of metabolites of interest during sample preparation can also result in a biased quantitative result (Vuckovic, 2012). To overcome this problem, we need to spike a fixed amount of the ^{13}C-labelled metabolite into each calibration sample (Mashego et al., 2004). Being chemically identical but having a different mass, this compound will be similarly ion suppressed within the matrix entering the mass spectrometer, but distinguished from unlabelled compound since its mass is slightly different. Therefore, the ratios of intensities of the ^{12}C-metabolite over the ^{13}C-metabolite are directly proportional to the concentrations of ^{12}C-metabolite. Using a calibration curve, the concentration of the metabolite can be determined in any sample if the same amount of ^{13}C-metabolite that has been used for the calibration curve is added to the sample. However, ^{13}C-labelled compounds are expensive and difficult to obtain. Therefore, uniformly (U)-^{13}C-labelled *E. coli* metabolite extracts, obtained by growing *E. coli* in M9 minimal medium with (U)-^{13}C-labelled glucose as the sole carbon source (Kiefer, Portais, & Vorholt, 2008), were

used as standards in the SilicoTryp project. This approach also offers the advantage that it potentially allows simultaneous quantification of all metabolites that can be detected in both *Escherichia coli* and *T. brucei*.

Using this method, we quantified 44 intracellular metabolites and 32 metabolites in the growth medium over a 57-h time course (starting from the low cell density of 3800 cells/ml to maintain the cells in exponential growth throughout the time course). Based on the 32 medium metabolite dynamics, we could quantify the fluxes of six metabolites that are constantly produced or consumed by the cells using the absolute concentrations and the cell densities at the same time points. Seven metabolites did not show any significant changes in concentration over time; for example, ornithine levels did not seem to change in the spent medium, which was unexpected since previous work had demonstrated that ornithine is taken up by the cells. Nineteen metabolites, all amino acids or nucleotides, showed changes of concentrations that are not compatible with constant production or consumption by the cells, but are compatible with the presence of peptidases and nucleosidases which degrade proteins and nucleic acids to their corresponding monomers. Indeed, it is known that *T. brucei* excretes peptidases and nucleosidases into the medium (Bossard, Cuny, & Geiger, 2013; Geiger et al., 2010; Knowles, Black, & Whitelaw, 1987).

From these results, and the ^{13}C-labelling experiments (see above), we could, for example, determine that about 2–3% of the pyruvate produced by cells grown in the simplified medium (Creek et al., 2013; see Section 5.2) is converted to alanine before being excreted. These results can now be used to extend the model and reduce our uncertainty about topology and parameter values.

5.2. Perturbations: RNAi cell lines

In order to provide information on the effect of reduced level of selected enzymes on the levels of mRNA, protein and the metabolome, we generated 28 stable RNA interference (RNAi) cell lines: 8 of them targeting genes of the polyamine pathway (the part of the trypanothione pathway that leads to the production of Spd in Fig. 3.7), 12 of the redox metabolism and 8 of the pentose phosphate pathway (see Table 3.2).

The RNAi cell lines were generated in monomorphic 2T1 *Trypanosoma brucei brucei*, selected among other available cell lines as it provides a unique target sequence at a single ribosomal RNA locus, and has been validated for robust inducible expression and has a higher RNAi efficiency (Alsford, Kawahara, Glover, & Horn, 2005). To confirm the specific down regulation

Table 3.2 List of RNAi mutants constructed and the previously published phenotypes

Gene ID	Protein	Growth reduction/ phenotype	References
Polyamine pathway			
Tb09.v1.0380	Spermidine synthase	Spermidine auxotrophy, depletion of $T(SH)_2$ and cell death	Xiao, McCloskey, and Phillips (2009)
Tb11.01.5300	Ornithine decarboxylase	Depletion of reduced thiols and cell growth arrest	Fairlamb, Henderson, Bacchi, and Cerami (1987)
Tb927.6.4410	*S*-adenosylmethionine decarboxylase	60–90%	Alsford et al. (2011)
Tb927.6.4470	Prozyme, activator of SAMDC	100%	Alsford et al. (2011)
Tb927.6.4840	Methionine adenosyltransferase	No effect	Alsford et al. (2011)
Tb927.6.4890	*S*-adenosylmethionine synthase	Unknown	Alsford et al. (2011)
Tb927.8.1910	Acetylornithine deacetylase	No effect	Alsford et al. (2011)
Pentose phosphate pathway and related enzymes			
Tb927.10.2490	Glucose-6-phosphate 1-dehydrogenase	Growth arrest, cell death	Cordeiro, Thiemann, and Michels (2009)
Tb11.02.4200	6-Phosphogluconolactonase	None	Alsford et al. (2011)
Tb09.211.3180	6-Phosphogluconate dehydrogenase	70–100%	Alsford et al., (2011)[a]
Tb927.8.6170	Transketolase	None	Alsford et al. (2011)
Tb927.10.12210	Ribulose-5-phosphate 3-epimerase	None	Alsford et al. (2011)
Tb11.03.0090	Ribokinase	70–80%	Alsford et al. (2011)

Continued

Table 3.2 List of RNAi mutants constructed and the previously published phenotypes—cont'd

Gene ID	Protein	Growth reduction/ phenotype	References
Tb927.4.1350	Glyoxalase II	20–80%	Alsford et al. (2011) and Wendler, Irsch, Rabbani, Thornalley, and Krauth-Siegel (2009)
Tb11.01.0700	Ribose 5-phosphate isomerase	>90%	Alsford et al. (2011)
Redox metabolism			
Tb927.3.3760	Tryparedoxin	Growth arrest and enhanced sensitivity against hydrogen peroxide	Alsford et al. (2011) and Comini, Krauth-Siegel, and Flohé (2007)
Tb09.160.2020	Thioredoxin	None	Alsford et al. (2011) and Schmidt, Clayton, and Krauth-Siegel (2002)
Tb927.2.4370	Trypanothione synthetase	Depletion of Gsp and $T(SH)_2$, growth arrest, loss of viability, enhanced sensitivity against hydroperoxides and drugs	Comini et al. (2004) and Ariyanayagam, Oza, Guther, and Fairlamb (2005)
Tb927.7.4000	Glutathione synthetase	10–80%	Alsford et al. (2011)
Tb927.10.12370	γ-Glutamylcysteine synthetase	Depletion of GSH and $T(SH)_2$, cell death and loss of virulence	Huynh, Huynh, Harmon, and Phillips (2003)

Table 3.2 List of RNAi mutants constructed and the previously published phenotypes—cont'd

Gene ID	Protein	Growth reduction/ phenotype	References
Tb927.10.10390	Trypanothione reductase	Growth arrest, loss of viability and virulence	Krieger et al. (2000)
Tb11.01.7560	Glutathione peroxidase, putative	>90%	Alsford et al. (2011)
Tb11.12.0016	Glutathionylspermidine synthetase	No effect	Alsford et al. (2011)
Tb09.160.4250	Peroxiredoxin-type tryparedoxin peroxidase (cytosolic)	Loss of viability and enhanced sensitivity against hydrogen peroxide	Alsford et al. (2011) and Wilkinson, Horn, Prathalingam, and Kelly (2003)
Tb927.4.2450	Protein disulfide isomerase I	15–60%	Alsford et al. (2011)
Tb927.3.4240	Thioredoxin, putative	40–80%	Alsford et al. (2011)
Tb927.5.950	Monothiol glutaredoxin 3	50–100%	Alsford et al. (2011)
Tb927.8.1990	Peroxiredoxin-type tryparedoxin peroxidase (mitochondrial)	None	Alsford et al., (2011) and Wilkinson et al. (2003)

[a]Kerkhoven et al. (2013).

of these enzymes at the protein level, RNAi cell lines where antibodies are available were selected, induced and tested by Western blot. So far, all RNAi lines tested by Western blot show down regulation of the protein of interest. The effects of ablating some of these enzymes have already been published, but most remain to be fully characterised (see Table 3.2). From the pentose phosphate pathway, only the glucose 6-phosphate 1-dehydrogenase (Cordeiro et al., 2009) and the 6-phosphogluconate dehydrogenase (Hanau, Rippa, Bertelli, Dallocchio, & Barrett, 1996) have been characterised previously.

Most of the evaluation of phenotypes in previous work has been carried out in a medium containing a vast excess of many metabolites. Comparing fresh and spent medium metabolomes revealed that most metabolites, however, are not consumed by trypanosomes. We therefore created a new medium from which those metabolites not consumed by trypanosomes were removed (Creek et al., 2013). Parasites grew equally well in this medium, which better reflects serum concentrations of many metabolites. Remarkably, experiments in the simplified medium revealed phenotypic effects that were hidden in the classical medium. For example, *T. brucei* bloodstream forms became over 100-fold more sensitive to antifolate drugs in the absence of the high concentrations of folate that are present in the classical medium (Creek et al., 2013).

The individual stable RNAi cell lines available now for each of our main genes of interest will allow us to confirm these results and also measure the changes in metabolites upon depletion of any particular enzyme as well as the effects, if any, on mRNA or protein levels of other enzymes. These perturbation responses will then inform the model debugging and refinement process.

6. CONCLUSION

The SilicoTryp project aimed at extending the core glycolysis model of the unicellular parasite *T. brucei* with the trypanothione pathway, and the translation and transcription of the enzymes involved. All of this work required newly developed modelling methods that explicitly take the multiple levels of biological and uncertainty into account. Hence, we first documented in detail the sources of the parameters of the existing core glycolysis model. This detailed information allowed us to re-evaluate this model taking our uncertainty about the parameter values into account (Achcar et al., 2012). In addition, we also questioned the topology of this model by analysing and comparing alternative possibilities (Achcar et al., 2013). These analyses formalised what our current levels of uncertainty are regarding the core glycolysis model. In the future, we aim at reducing these uncertainties using Bayesian inference methods, which use new experimental data to update our belief on parameter values and model topology (see Fig. 3.1). Because of the complexity of the models we are dealing with, we developed a new state-of-the-art variance reduction method specifically for this purpose (Papamarkou et al., 2014).

Although modelling attempts have been made for part of this pathway both in *T. brucei* (Gu, Reid, Higham, & Gilbert, 2013) and *T. cruzi* (Olin-Sandoval et al., 2012), working towards the introduction of the trypanothione pathway introduced a new set of challenges. First, introducing the pentose phosphate pathway, the link between glycolysis and the trypanothione pathway, revealed new uncertainties about the topology of this pathway in *T. brucei*. We were nevertheless able to predict relevant behaviours of the system based on the alternative versions of the model (Kerkhoven et al., 2013). Then, to be able to introduce the trypanothione pathway *per se*, we again had to clarify some topological questions. We were able to do so using ^{13}C-labelled metabolites and LC–MS. For example, we showed that MTA is not recycled to methionine in *T. brucei*. However, deciphering the origin of ornithine *in vivo* will require further investigation. In addition to investigating the topology of this pathway, new kinetic parameters of the enzymes involved have to be measured. To reduce our uncertainty about this new kinetics, we designed a new *in vivo*-like buffer. Using this new assay system and a method based on a strong interaction between modellers and experimentalists, we deciphered in detail the complex mechanism of the trypanothione synthetase, the last enzyme of the trypanothione biosynthesis pathway (Leroux et al., 2013).

Introducing the possibility of dynamic regulation to these pathways at the transcriptional and translational levels requires new sets of parameters that have to be measured using specific methodologies. These regulatory steps will be introduced to the models using a module of four differential equations based on the previously published model of PGK transcription and translation (Haanstra, Stewart, et al., 2008). We designed appropriate methodology to measure the parameters needed based on deep sequencing (RNAseq).

All of these new additions introduced many new parameters and additional topological uncertainties. To enable reduction of these uncertainties using a Bayesian methodology, we collected additional data about metabolite concentrations and fluxes, using a new method based on LC–MS data. Intracellular and extracellular concentrations and fluxes were collected in the wild type cell line. In the future, we also plan to collect metabolite concentrations in mutant cell lines to produce new information about the system under perturbation. Therefore, 28 RNAi cell lines targeting critical enzymes in our system were constructed and verified. We will now be able to grow these cell lines in uniform controlled conditions to characterise the metabolomic and transcriptomic response to these perturbations.

This work opens many novel perspectives: our main aim now is to apply our newly developed Bayesian inference methods to our models and data, starting with small models and gradually increasing model size. While the first small models will be analysed, new enzymes kinetics will be acquired, but also the deep sequencing data will be analysed and the RNAi mutants studied. Each additional dataset acquired will allow us to reduce our uncertainty on some part of the model. We argue that the conceptual framework we are developing here to study the metabolism of *T. brucei*, including the explicit quantitative consideration of topological and parameter uncertainty, can be applied to study any biological system and offers powerful new approaches to enable the robust and predictive simulation of cellular function.

ACKNOWLEDGEMENTS

This work was supported by the Scottish Universities Life Sciences Alliance (SULSA), the Federal Ministry of Education and Research (Germany), the Netherlands Organisation for Scientific Research (NWO, The Netherlands) and the Biotechnology and Biological Sciences Research Council (BBSRC, United Kingdom), within the framework of the SysMO2-funded SilicoTryp project. BMB received a Rosalind Franklin Fellowship from the University of Groningen.

REFERENCES

Achcar, F., Barrett, M. P., & Breitling, R. (2013). Explicit consideration of topological and parameter uncertainty gives new insights into a well-established model of glycolysis. *The FEBS Journal*, *280*, 4640–4651.

Achcar, F., Kerkhoven, E. J., Bakker, B. M., Barrett, M. P., & Breitling, R. The SilicoTryp Consortium. (2012). Dynamic modelling under uncertainty: The case of *Trypanosoma brucei* energy metabolism. *PLoS Computational Biology*, *8*(1), e1002352.

Albert, M. A., Haanstra, J. R., Hannaert, V., Van Roy, J., Opperdoes, F. R., Bakker, B. M., et al. (2005). Experimental and in silico analyses of glycolytic flux control in bloodstream form *Trypanosoma brucei*. *Journal of Biological Chemistry*, *280*(31), 28306–28315.

Alsford, S., Kawahara, T., Glover, L., & Horn, D. (2005). Tagging a T. brucei RRNA locus improves stable transfection efficiency and circumvents inducible expression position effects. *Molecular and Biochemical Parasitology*, *144*(2), 142–148.

Alsford, S., Turner, D. J., Obado, S. O., Sanchez-Flores, A., Glover, L., Berriman, M., et al. (2011). High-throughput phenotyping using parallel sequencing of RNA interference targets in the African trypanosome. *Genome Research*, *21*(6), 915–924.

Annesley, T. M. (2003). Ion suppression in mass spectrometry. *Clinical Chemistry*, *49*(7), 1041–1044.

Ariyanayagam, M. R., Oza, S. L., Guther, M. L. S., & Fairlamb, A. H. (2005). Phenotypic analysis of trypanothione synthetase knockdown in the African trypanosome. *The Biochemical Journal*, *391*(Pt 2), 425–432.

Bakker, B. M., Mensonides, F. I., Teusink, B., van Hoek, P., Michels, P. A. M., & Westerhoff, H. V. (2000). Compartmentation protects trypanosomes from the

dangerous design of glycolysis. *Proceedings of the National Academy of Sciences of the United States of America*, *97*(5), 2087–2092.

Bakker, B. M., Michels, P. A. M., Opperdoes, F. R., & Westerhoff, H. V. (1997). Glycolysis in bloodstream form *Trypanosoma brucei* can be understood in terms of the kinetics of the glycolytic enzymes. *Journal of Biological Chemistry*, *272*(6), 3207–3215.

Bakker, B. M., Michels, P. A. M., Opperdoes, F. R., & Westerhoff, H. V. (1999). What controls glycolysis in bloodstream form *Trypanosoma brucei*? *Journal of Biological Chemistry*, *274*(21), 14551–14559.

Bakker, B. M., Walsh, M. C., ter Kuile, B. H., Mensonides, F. I. C., Michels, P. A. M., Opperdoes, F. R., et al. (1999). Contribution of glucose transport to the control of the glycolytic flux in *Trypanosoma brucei*. *Proceedings of the National Academy of Sciences of the United States of America*, *96*(18), 10098–10103.

Barrett, M. P., Bakker, B. M., & Breitling, R. (2010). Metabolomic systems biology of trypanosomes. *Parasitology*, *137*(9), 1285–1290.

Barrett, M. P., Burchmore, R. J. S., Stich, A., Lazzari, J. O., Frasch, A. C., Cazzulo, J. J., et al. (2003). The trypanosomiases. *Lancet*, *362*(9394), 1469–1480.

Bossard, G., Cuny, G., & Geiger, A. (2013). Secreted proteases of *Trypanosoma brucei gambiense*: Possible targets for sleeping sickness control? *Biofactors*, *39*, 407–414.

Breitling, R., Achcar, F., & Takano, E. (2013). Modeling challenges in the synthetic biology of secondary metabolism. *ACS Synthetic Biology*, *2*(7), 373–378.

Comini, M. A., Guerrero, S. A., Haile, S., Menge, U., Lünsdorf, H., & Flohé, L. (2004). Validation of *Trypanosoma brucei* trypanothione synthetase as drug target. *Free Radical Biology and Medicine*, *36*(10), 1289–1302.

Comini, M. A., Krauth-Siegel, R. L., & Flohé, L. (2007). Depletion of the thioredoxin homologue tryparedoxin impairs antioxidative defence in African trypanosomes. *The Biochemical Journal*, *402*(1), 43–49.

Cordeiro, A. T., Thiemann, O. H., & Michels, P. A. M. (2009). Inhibition of *Trypanosoma brucei* glucose-6-phosphate dehydrogenase by human steroids and their effects on the viability of cultured parasites. *Bioorganic and Medicinal Chemistry*, *17*(6), 2483–2489.

Creek, D. J., Nijagal, B., Kim, D. H., Rojas, F., Matthews, K. R., & Barrett, M. P. (2013). Metabolomics guides rational development of a simplified cell culture medium for drug screening against *Trypanosoma brucei*. *Antimicrobial Agents and Chemotherapy*, *57*(6), 2768–2779.

Deneke, C., Lipowsky, R., & Valleriani, A. (2013). Complex degradation processes lead to non-exponential decay patterns and age-dependent decay rates of messenger RNA. *PLoS One*, *8*(2), e55442.

Fadda, A., Färber, V., Droll, D., & Clayton, C. (2013). The roles of 3′-exoribonucleases and the exosome in trypanosome mRNA degradation. *RNA*, *19*(7), 937–947.

Fairlamb, A. H., Henderson, G. B., Bacchi, C. J., & Cerami, A. (1987). In vivo effects of difluoromethylornithine on trypanothione and polyamine levels in bloodstream forms of *Trypanosoma brucei*. *Molecular and Biochemical Parasitology*, *24*(2), 185–191.

Fuad, F. A. A., Fothergill-Gilmore, L. A., Nowicki, M. W., Eades, L. J., Morgan, H. P., McNae, I. W., et al. (2011). Phosphoglycerate mutase from *Trypanosoma brucei* is hyperactivated by cobalt *in vitro*, but not *in vivo*. *Metallomics*, *3*(12), 1310–1317.

Geiger, A., Hirtz, C., Bécue, T., Bellard, E., Centeno, D., Gargani, D., et al. (2010). Exocytosis and protein secretion in Trypanosoma. *BMC Microbiology*, *10*, 20.

Gu, X., Reid, D., Higham, D. J., & Gilbert, D. (2013). Mathematical modelling of polyamine metabolism in bloodstream-form *Trypanosoma brucei*: An application to drug target identification. *PLoS One*, *8*(1), e53734.

Gualdron-López, M., Vapola, M. H., Miinalainen, I. J., Hiltunen, J. K., Michels, P. A. M., & Antonenkov, V. D. (2012). Channel-forming activities in the glycosomal fraction from the bloodstream form of *Trypanosoma brucei*. *PLoS One*, *7*(4), e34530.

Haanstra, J. R., Stewart, M., Luu, V. D., van Tuijl, A., Westerhoff, H. V., Clayton, C., et al. (2008). Control and regulation of gene expression: Quantitative analysis of the expression of phosphoglycerate kinase in bloodstream form *Trypanosoma brucei*. *Journal of Biological Chemistry*, *283*(5), 2495–2507.

Haanstra, J. R., van Tuijl, A., Kessler, P., Reijnders, W., Michels, P. A. M., Westerhoff, H. V., et al. (2008). Compartmentation prevents a lethal turbo-explosion of glycolysis in trypanosomes. *Proceedings of the National Academy of Sciences of the United States of America*, *105*(46), 17718–17723.

Hanau, S., Rippa, M., Bertelli, M., Dallocchio, F., & Barrett, M. P. (1996). 6-Phosphogluconate dehydrogenase from *Trypanosoma brucei*. Kinetic analysis and inhibition by trypanocidal drugs. *European Journal of Biochemistry*, *240*(3), 592–599.

Häusler, T., Stierhof, Y. D., Wirtz, E., & Clayton, C. (1996). Import of a DHFR hybrid protein into glycosomes in vivo is not inhibited by the folate-analogue aminopterin. *Journal of Cell Biology*, *132*(3), 311–324.

Helfert, S., Estévez, A. M., Bakker, B., Michels, P., & Clayton, C. (2001). Roles of triosephosphate isomerase and aerobic metabolism in *Trypanosoma brucei*. *The Biochemical Journal*, *357*(Pt 1), 117–125.

Huynh, T. T., Huynh, V. T., Harmon, M. A., & Phillips, M. A. (2003). Gene knockdown of gamma-glutamylcysteine synthetase by RNAi in the parasitic protozoa *Trypanosoma brucei* demonstrates that it is an essential enzyme. *Journal of Biological Chemistry*, *278*(41), 39794–39800.

Ingolia, N. T., Ghaemmaghami, S., Newman, J. R. S., & Weissman, J. S. (2009). Genome-wide analysis in vivo of translation with nucleotide resolution using ribosome profiling. *Science*, *324*(5924), 218–223.

Kerkhoven, E. J., Achcar, F., Alibu, V. P., Burchmore, R. J., Gilbert, I. H., Trybiło, M., et al. (2013). Handling uncertainty in dynamic models: the pentose phosphate pathway in *Trypanosoma brucei*. *PLoS Computational Biolog*, *9*(12), e1003371.

Kiefer, P., Portais, J. C., & Vorholt, J. A. (2008). Quantitative metabolome analysis using liquid chromatography-high-resolution mass spectrometry. *Analytical Biochemistry*, *382*(2), 94–100.

Knowles, G., Black, S. J., & Whitelaw, D. D. (1987). Peptidase in the plasma of mice infected with *Trypanosoma brucei brucei*. *Parasitology*, *95*(Pt 2), 291–300.

Krieger, S., Schwarz, W., Ariyanayagam, M. R., Fairlamb, A. H., Krauth-Siegel, R. L., & Clayton, C. (2000). Trypanosomes lacking trypanothione reductase are avirulent and show increased sensitivity to oxidative stress. *Molecular Microbiology*, *35*(3), 542–552.

Leroux, A. E., Haanstra, J. R., Bakker, B. M., & Krauth-Siegel, R. L. (2013). Dissecting the catalytic mechanism of *Trypanosoma brucei* trypanothione synthetase by kinetic analysis and computational modelling. *The Journal of Biological Chemistry*, *288*, 23751–23764.

Martens-Lobenhoffer, J., Postel, S., Tröger, U., & Bode-Böger, S. M. (2007). Determination of ornithine in human plasma by hydrophilic interaction chromatography–tandem mass spectrometry. *Journal of Chromatography B: Analytical Technologies in the Biomedical and Life Sciences*, *855*(2), 271–275.

Mashego, M. R., Wu, L., Van Dam, J. C., Ras, C., Vinke, J. L., Van Winden, W. A., et al. (2004). MIRACLE: Mass isotopomer ratio analysis of u-13C-labeled extracts. A new method for accurate quantification of changes in concentrations of intracellular metabolites. *Biotechnology and Bioengineering*, *85*(6), 620–628.

Michels, R. A. M., Moyersoen, J., Krazy, H., Galland, N., Herman, M., & Hannaert, V. (2005). Peroxisomes, glyoxysomes and glycosomes (review). *Molecular Membrane Biology*, *22*(1–2), 133–145.

Moreno, B., Urbina, J. A., Oldfield, E., Bailey, B. N., Rodrigues, C. O., & Docampo, R. (2000). ^{31}P NMR spectroscopy of *Trypanosoma brucei*, *Trypanosoma cruzi*, and *Leishmania major*: Evidence for high levels of condensed inorganic phosphates. *Journal of Biological Chemistry*, *275*(37), 28356–28362.

Nolan, D. P., & Voorheis, H. P. (2000a). Hydrogen ion gradients across the mitochondrial, endosomal and plasma membranes in bloodstream forms of *Trypanosoma brucei* solving the three-compartment problem. *European Journal of Biochemistry*, *267*(15), 4601–4614.

Nolan, D. P., & Voorheis, H. P. (2000b). Factors that determine the plasma-membrane potential in bloodstream forms of *Trypanosoma brucei*. *European Journal of Biochemistry*, *267*(15), 4615–4623.

Olin-Sandoval, V., González-Chávez, Z., Berzunza-Cruz, M., Martínez, I., Jasso-Chávez, R., Becker, I., et al. (2012). Drug target validation of the trypanothione pathway enzymes through metabolic modelling. *The FEBS Journal*, *279*(10), 1811–1833.

Oza, S. L., Ariyanayagam, M. R., Aitcheson, N., & Fairlamb, A. H. (2003). Properties of trypanothione synthetase from *Trypanosoma brucei*. *Molecular and Biochemical Parasitology*, *131*(1), 25–33.

Papamarkou, T., Mira, A., & Girolami, M. (2014). Zero variance differential geometric Markov Chain Monte Carlo algorithms. *Bayesian Analysis*, *9*(1), 97–128.

Schmidt, A., Clayton, C. E., & Krauth-Siegel, R. L. (2002). Silencing of the thioredoxin gene in Trypanosoma brucei brucei. *Molecular and Biochemical Parasitology*, *125*(1–2), 207–210.

Siegel, T. N., Gunasekera, K., Cross, G. A. M., & Ochsenreiter, T. (2011). Gene expression in *Trypanosoma brucei*: Lessons from high-throughput RNA sequencing. *Trends in Parasitology*, *27*(10), 434–441.

Thissen, J. A., & Wang, C. C. (1991). Maintenance of internal pH and an electrochemical gradient in *Trypanosoma brucei*. *Experimental Parasitology*, *72*(3), 243–251.

Torrie, L. S., Wyllie, S., Spinks, D., Oza, S. L., Thompson, S., Harrison, J. R., et al. (2009). Chemical validation of trypanothione synthetase: A potential drug target for human trypanosomiasis. *Journal of Biological Chemistry*, *284*(52), 36137–36145.

van Eunen, K., Bouwman, J., Daran-Lapujade, P., Postmus, J., Canelas, A. B., Mensonides, F. I. C., et al. (2010). Measuring enzyme activities under standardized in vivo-like conditions for systems biology. *The FEBS Journal*, *277*(3), 749–760.

van Eunen, K., Kiewiet, J. A. L., Westerhoff, H. V., & Bakker, B. M. (2012). Testing biochemistry revisited: How in vivo metabolism can be understood from in vitro enzyme kinetics. *PLoS Computational Biology*, *8*(4), e1002483.

Vincendeau, P., Gobert, A. P., Daulouède, S., Moynet, D., & Djavad Mossalayi, M. (2003). Arginases in parasitic diseases. *Trends in Parasitology*, *19*(1), 9–12.

Vincent, I. M., Creek, D. J., Burgess, K., Woods, D. J., Burchmore, R. J. S., & Barrett, M. P. (2012). Untargeted metabolomics reveals a lack of synergy between nifurtimox and eflornithine against Trypanosoma brucei. *PLoS Neglected Tropical Diseases*, *6*(5), e1618.

Vuckovic, D. (2012). Current trends and challenges in sample preparation for global metabolomics using liquid chromatography-mass spectrometry. *Analytical and Bioanalytical Chemistry*, *403*(6), 1523–1548.

Vyshemirsky, V., & Girolami, M. A. (2008). Bayesian ranking of biochemical system models. *Bioinformatics*, *24*(6), 833–839.

Wendler, A., Irsch, T., Rabbani, N., Thornalley, P. J., & Krauth-Siegel, R. L. (2009). Glyoxalase II does not support methylglyoxal detoxification but serves as a general trypanothione thioesterase in African trypanosomes. *Molecular and Biochemical Parasitology*, *163*(1), 19–27.

Wilkinson, S. R., Horn, D., Prathalingam, S. R., & Kelly, J. M. (2003). RNA interference identifies two hydroperoxide metabolizing enzymes that are essential to the bloodstream form of the African trypanosome. *Journal of Biological Chemistry*, *278*(34), 31640–31646.

Xiao, Y., McCloskey, D. E., & Phillips, M. A. (2009). RNA interference-mediated silencing of ornithine decarboxylase and spermidine synthase genes in *Trypanosoma brucei* provides insight into regulation of polyamine biosynthesis. *Eukaryotic Cell*, *8*(5), 747–755.

Xu, T. R., Vyshemirsky, V., Gormand, A., von Kriegsheim, A., Girolami, M., Baillie, G. S., et al. (2010). Inferring signaling pathway topologies from multiple perturbation measurements of specific biochemical species. *Science Signaling*, *3*(113), ra20.